(9) Mikkelsen, R. B. In "Biological Membranes", Chapman, D., Wallach, D. F. H., Eds.; Academic Press: New York, 1976; Vol. 3, p 152.
(10) Nieboer, E. *Struct. Bonding (Berlin)* **1975**, *22*, 1.
(11) Ellis, K. J. *Inorg. Perspect. Biol. Med.* **1977**, *1*, 101.
(12) Reuben, J. *J. Am. Chem. Soc.* **1975**, *97*, 3823.
(13) Lewis, B. A.; Freyssinet, J.; Holbrook, J. J. *Biochem. J.* **1978**, *169*, 397.
(14) Horrocks, Jr., W. DeW.; Sudnick, D. R. *J. Am. Chem. Soc.* **1979**, *101*, 334.
(15) Horrocks, Jr., W. DeW.; Schmidt, G. F.; Sudnick, D. R.; Kittrell, C.; Bernheim, R. A. *J. Am. Chem. Soc.* **1977**, *99*, 2378.
(16) Mann, K. G. *Methods Enzymol.* **1976**, *45*, 123-156.
(17) Sarasua, M. M.; Scott, M. E.; Helpern, J. A.; Ten Kortenaar, P. B. W.; Boggs, N. T. III; Pedersen, L. G.; Koehler, K. A.; Hiskey, R. G., *J. Am. Chem. Soc.*, preceding paper in this issue.
(18) Marshall, A. G.; Hall, L. D.; Hatton, M.; Sallos, J. *J. Magn. Reson.* **1974**, *13*, 392.
(19) Furie, B. C.; Mann, K. G.; Furler, B. *J. Biol. Chem.* **1976**, *251*, 3235.
(20) Brittain, H. G.; Richardson, F. S.; Martin, R. B. *J. Am. Chem. Soc.* **1976**, *98*, 8255.
(21) Scott, M. E.; Koehler, K. A.; Hiskey, R. G. *Biochem. J.* **1979**, *177*, 679.
(22) Madar, D. A.; Willis, R. A.; Koehler, K. A.; Hiskey, R. G. *Anal. Biochem.* **1979**, *92*, 466.
(23) Reuben, J.; Luz, Z. *J. Phys. Chem.* **1976**, *80*, 1357.
(24) Hubbard, P. S. *J. Chem. Phys.* **1970**, *53*, 985.
(25) Hubbard, P. S. *Phys. Rev. A* **1974**, *9*, 481.
(26) James, T. L. "Nuclear Magnetic Resonance in Biochemistry"; Academic Press: New York, 1975; p 60.
(27) Epstein, M.; Reuben, J.; Levitzki, A. *Biochemistry* **1977**, *16*, 2449.
(28) Reuben, J. *Biochemistry* **1971**, *10*, 2834.
(29) Jones, R.; Dwek, R. A.; Forsen, S. *Eur. J. Biochem.* **1974**, *47*, 271.
(30) Fuller, L. D.; LaFond, R. E. *Biochemistry* **1971**, *10*, 1033.
(31) Shaw, D. "Fourier Transform NMR Spectroscopy"; Elsevier: Amsterdam, 1976; p 315.
(32) Robertson, Jr., P.; Koehler, K. A.; Hiskey, R. G. *Biochem. Biophys. Res. Commun.* **1979**, *86*, 265.
(33) Marki, W.; Oppliger, M.; Thanei, P.; Schwyzer, R. *Helv. Chim. Acta* **1977**, *60*, 798.
(34) Sperling, R.; Furie, B. C.; Blemenstein, M.; Keyt, B.; Furie, B. *J. Biol. Chem.* **1978**, *253*, 3898-3906.
(35) Abbreviations: fragment 1 (F-1), amino terminal portion of prothrombin released upon treatment of prothrombin with thrombin; Gla, γ-carboxyglutamic acid; EDTA, ethylenediaminetetraacetic acid; Tris, tris(hydroxymethyl)aminomethane; MES, *N*-morpholinoethanesulfonic acid; NMR, nuclear magnetic resonance.

Paramagnetic Carbon Monoxide on Magnesium Oxide

R. M. Morris, R. A. Kaba, T. G. Groshens, K. J. Klabunde,*[1] R. J. Baltisberger, N. F. Woolsey, and V. I. Stenberg

Contribution from the Department of Chemistry, University of North Dakota, Grand Forks, North Dakota 58202. *Received July 2, 1979*

Abstract: Upon exposure of thermally activated MgO to CO, a paramagnetic species is produced at room temperature. A variety of experiments have been carried out in order to elucidate the nature of the CO radical: (1) EPR ^{13}CO experiments with computer simulation indicate that the radical is dimeric; (2) infrared experiments indicate that the radical is anion-like rather than cation-like, and reveal the presence of other CO telomeric species; (3) comparisons of CO/MgO with $C_6H_5NO_2$/MgO reveal that similar sites on MgO are necessary to produce the radical-anion-like species in each case.

Introduction

The electron transfer surface chemistry of MgO can be enhanced by two types of activation procedures:[2,3] (1) High-energy irradiation (neutron, X-rays, or ultraviolet irradiation) causes white MgO to turn blue to red-blue. The color is due to the formation of free electrons which are trapped in crystalline defects which are then called paramagnetic F centers (bulk defects) or S centers (surface defects). When small molecules such as O_2,[4] N_2O,[4] CO_2,[5] SO_2,[6] and H_2S[7] are exposed to this activated, colored MgO, stabilized paramagnetic radical anions are formed, such as $O_2^{-}\cdot$, etc. Such radical anions have been probed by ESR techniques.[4-7] (2) Thermal activation by heating under vacuum from 400 to 1000 °C causes the surface of MgO to become susceptible to electron-transfer processes, but no F or S centers are formed. Adsorbed electron-demanding molecules may become paramagnetic, however. For example, aromatic nitro compounds adsorbed on thermally activated MgO surfaces have been reported to yield the corresponding radical anions.[8,9] Tench and Nelson attributed this surface electron transfer activity to the presence of coordinately unsaturated O^{2-} centers. Cordischi and co-workers have reported the formation of two nitrobenzene radicals on MgO, $C_6H_5NO_2^{-}\cdot$ and $C_6H_5\dot{N}O_2H$, the latter species apparently formed by protonation of the radical anion by surface OH groups.[9]

For strongly electron-demanding molecules, such as nitrobenzene, *p*-nitrotoluene, *p*-fluoronitrobenzene, and tetracyanoethylene, there appears to be little correlation between actual electron affinity and concentration of radical anions formed on the MgO surface.[9-11] This finding is most readily explained by noting our previous report showing that nitrobenzene actually forms a *monolayer* of radical anion species on MgO, and steric limitations prevent the addition of more molecules.[12] This is probably the case for all molecules of such high electron affinity.

Molecules of much lower electron affinity exhibit significantly different behavior. Electron-transfer processes do occur, but with apparently much greater selectivity for certain types of surface defects.[12] For example, Lunsford and Jayne[13] reported in 1966 that well-degassed thermally activated MgO interacted with CO at room temperature to produce a paramagnetic species which was believed to be bonded to the surface in a manner similar to the bonding of metal carbonyls.[14] The EPR spectrum of this radical species exhibited an axially symmetric g value ($g_\perp = 2.0055$, $g_\parallel = 2.0021$).[13]

In this study three methods have been employed for investigation of the CO radical species: (1) comparisons of activities of a series of thermally activated MgO samples for radical formation (anion radical) with nitrobenzene vs. carbon monoxide; (2) infrared studies of CO adsorbed on thermally activated MgO samples; and (3) studies of adsorbed ^{13}CO on MgO samples employing extensive computer simulation techniques.

Experimental Section

Materials. For most of the results a sample of 99.99% MgO from ROC/RIC (labeled MgO I) was used. Other samples include a second lot of 99.99% MgO from ROC/RIC (MgO II), a 99.9% MgO sample from ROC/RIC (MgO III), and a Fischer reagent grade power (MgO

0002-7863/80/1502-3419$01.00/0

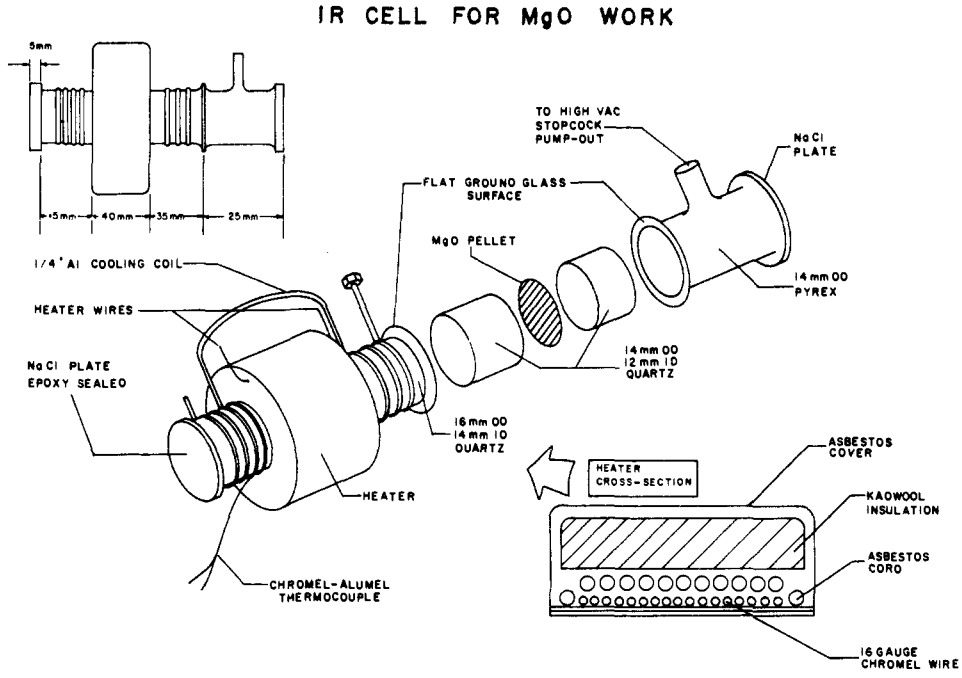

Figure 1. Design of an infrared cell for study of thermally activated alkaline earth oxides.

IV). Surface areas were determined by the BET method. The iron content of the several samples was determined by a spectrophotometric method.[15] The following results were obtained: MgO I, 0.0018% Fe; MgO II, 0.0036% Fe; MgO III, 0.0016% Fe; MgO IV, 0.0013% Fe. Prior to thermal activation, samples were boiled in distilled H_2O for several hours and then dried at ca. 120 °C overnight in air.

Carbon-12 carbon monoxide was Matheson Research Grade (99.99%) and was passed through a liquid-nitrogen trap prior to contact with the MgO surface. Labeled ^{13}CO was obtained from Prochem (Summit, N.J.) and was 97% ^{13}CO as indicated by mass-spectrometric analysis. The gas was slowly passed through a 20-cm column packed with BASF catalyst R3-11 operated at ca. 100 °C, and then through a liquid-nitrogen trap before contact with the MgO. This procedure was performed in order to remove ca. 0.4% O_2 contamination present in the reagent vessel.

Nitrobenzene (Eastman reagent grade) was purified by several vacuum distillations, degassed by several freeze-thaw-freeze cycles, and then placed under vacuum at ca. −20 °C to remove CO_2.

Sample Preparation. Samples (20-200 mg) were normally contained in quartz EPR tubes fitted with a stopcock, and were heat treated under vacuum at the desired temperature overnight (ca. 16 h). Final pressure was normally 2×10^{-6} to 5×10^{-7} Torr, the pressure generally attained in studies of this type.[2-13,17] The samples were then cooled to room temperature before exposure to CO. In order to determine the total amount of CO adsorbed the sample size was increased to ca. 1.5 g and a coarse glass frit was placed between the sample and the vacuum system to prevent the loss of powder while pumping. For the CO work the degassed surface was exposed to ca. 150 Torr CO and the CO atmosphere was not removed. For a few samples the atmosphere was removed after ca. 5 min CO exposure. Nitrobenzene vapor (vapor pressure at room temperature) was allowed to contact the surface until a uniform color (yellow-brown) developed (usually ca. 15 min). After 2 days excess nitrobenzene was removed under vacuum.

EPR Spectroscopy. A Bruker ER-420/10V EPR spectrometer operating in the X-band with 100-kHz field modulation and equipped with a double cavity was used. The g values were determined by direct comparison with aqueous potassium peroxylamine disulfonate (g value of 2.0055). For unsymmetrical EPR signals the g values were determined using the Kneubühl method.[16] For the relative radical concentration determinations in the MgO/CO system the height from the base line of the high-field component of the CO radical species EPR signal was measured relative to the height of a Mn^{2+} impurity line in a standard MgO sample. The high-field component was used rather than the total signal because of low-field shoulders that have been shown[13] to be due to O_2 contamination. The problem with O_2 was most acute at the lower heat treatment temperatures. In the MgO/nitrobenzene samples the relative radical concentrations were determined by numerical double integration of the total signal vs. a 10^{-4} M benzene solution of 1,1-diphenylpicrylhydrazine (DPPH). A solid, dilute mixture of DPPH in KCl was used to determine the absolute number of spins in several samples of both the CO and nitrobenzene systems using a numerical double integration technique. The sample and reference were interchanged to correct for differences in sample positions. The microwave power was kept low (ca. 1 mW) to avoid saturation. The remainder of the relative data could then be converted to absolute number of spins data.

Computer Simulations. An EPR line shape synthesis program called FIBRE was used to aid in the determination of the hyperfine splitting constants in the carbon-13 carbon monoxide spectrum.[17] An IBM-370/148 was used for computations and a Digital DecwriterII was used as the output device.

Infrared Studies. Pellets of MgO were prepared from MgO (before heat treatment) by using a normal KBr pellet press. A very thin pellet (ca. 30 mg) was placed in an infrared cell of a special design (Figure 1). The sample could be heat treated under vacuum followed by cooling to room temperature and addition of 150 Torr CO. After the pellet was aged in a CO atmosphere for the desired length of time, the CO was removed under vacuum and an IR spectrum recorded on a Beckman IR-12 instrument. If desired, CO could again be added and further aging allowed to continue.

Results and Discussion

I. Comparison of CO with $C_6H_5NO_2$ on MgO. Since it is known that for $C_6H_5NO_2$ an anion radical is formed on the MgO surface,[8,9] we believed that, if similar MgO activities for CO radical formation and $C_6H_5NO_2^-\cdot$ formation were found, this would be an indication that the CO radical is anion-radical-like. Previous work has indicated that the thermal activation temperature for MgO affects the relative populations of different crystalline faces on the surface,[18] and so the number of defects and/or active sites for $C_6H_5NO_2^-\cdot$ formation and CO radical formation should be affected. In accordance with this idea, portions of a single MgO sample were heat treated under vacuum at a series of temperatures, and surface areas determined by the BET method yielding the following values: 300 °C, 83 m^2/g; 400 °C, 213 m^2/g; 500 °C, 139 m^2/g; 600 °C, 140 m^2/g; 700 °C, 130 m^2/g; 800 °C, 134 m^2/g; 900 °C, 129 m^2/g; 1000 °C, 122 m^2/g.

Figure 2 illustrates that a change in thermal activation temperature from 500 to 1000 °C causes a very significant change in the rate of CO radical formation, as well as a change

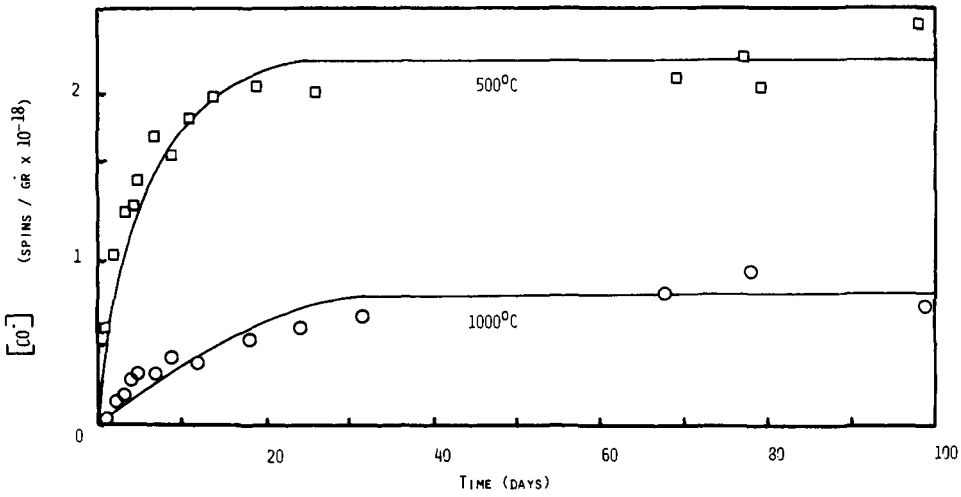

Figure 2. Representative curves for the growth of the CO radical EPR signal at room temperature in the MgO/CO system with time at several heat treatment temperatures. One sample was heat treated at 500 °C (-□-) and the other at 1000 °C (-○-).

in the final surface concentration of these radicals. Furthermore, Figure 3 illustrates that there is a trend in activity change (with change in thermal activation temperature) and that this trend is the *same for radical formation from CO and* $C_6H_5NO_2$. The highest activities (final concentrations) were found for samples pretreated at 500 °C, and this activity fell and leveled off on moving to high pretreatment temperatures. These results cannot be due to surface area effects since the surface area of a sample previously heated to 500 °C is essentially the same as that of the higher pretreatment samples.

II. Infrared Studies of ^{12}CO on MgO. Since we had previously determined that in our ^{12}CO/MgO EPR studies at least 15% of the adsorbed CO (at 25 °C) was in a paramagnetic form after appropriate aging of the sample (about 2 weeks),[12] we considered it possible to detect this species by infrared spectroscopy. Thus, a sample cell was built that allowed the treatment of thin MgO pellets (wafers) with high temperature and vacuum followed by cooling and inletting of CO. The CO (150 Torr) was immediately removed under vacuum and a spectrum recorded. Then the CO was replaced and the sample allowed to age. Spectra were recorded intermittently over 1 month by vacuum removal of CO and, after recording, the CO was replenished. Figure 4 illustrates the total spectrum of an aged sample. Note the great number of bands with $\nu_{C=O}$ absorptions spanning the 1000-2200-cm^{-1} range. This indicates that there is a wide variety of chemically different adsorbed CO species present. The high-energy absorption at 2110 cm^{-1} probably is due to physisorbed CO, while the very low absorptions in the 1500-100-cm^{-1} region probably are due to polymeric rings of CO on the surface first suggested by Zecchina and Stone based on UV-visible studies.[19] Our preliminary results indicate that many of these IR-detectable species can be selectively desorbed by slow heating, or selectively destroyed chemically, for example, with O_2.

Overall, our results are in good agreement with the recent findings of Zecchina and co-workers.[20] Their very interesting IR work indicated, among other things, that many of the adsorbed species are CO clusters of the type $(CO)_n^{x-}$ where $x = 2$ or 4 and $n = 2$. They proposed that formation of these species may involve surface disproportionation processes with coordinatively unsaturated O^{2-} as a key reactant.[20]

The Zecchina work and our work clearly illustrate that there are several types of adsorbed species on MgO. However, our EPR work, employing selective microwave saturation, selective desorption, and spectra simulation, indicates that only one of these species is paramagnetic in nature.

Figure 5 illustrates a series of IR absorptions in the

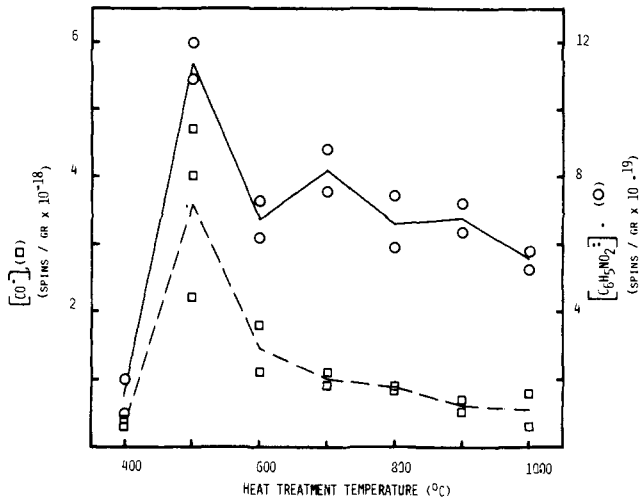

Figure 3. Radical concentration in both the MgO/CO (- -□- -) and MgO/nitrobenzene (-○-) systems as a function of the MgO heat treatment temperature. The ordinate scales for the two systems differ by a factor of 10.

1900-1500-cm^{-1} region which were present after short exposure of the heat-treated MgO pellet to CO. Upon aging many of the bands increased slightly in intensity. However, only in the 1710-1740-cm^{-1} region was there any significant change during the aging process. In about 2 days a band at 1714 cm^{-1} grew in and in about 7-9 days a band at 1733 cm^{-1} grew in. The 1733 cm^{-1} band growth corresponds reasonably well with the rate of growth of the CO radical according to EPR (most growth has occurred in the first 10 days). These EPR and IR experiments were carried out under exactly the same temperature and vacuum conditions. Furthermore, the appearance of the samples according to color changes was very similar as the two sets of experiments progressed. Finally, very good reproducibility in these growth patterns was found.

Thermal treatment under vacuum of the aged MgO-CO samples revealed that at 150 °C the 1714-cm^{-1} band disappeared while the 1733-cm^{-1} band disappeared at 205-240 °C. Again, comparison with EPR desorption data is of interest in that the CO radical in unaffected at 150 °C, but its EPR signal disappears between 150 and 250 °C.

Treatment of aged MgO-CO samples with small amounts of oxygen was also informative. Addition of 1.5-200 μ pressure of O_2 slowly caused the 1733-cm^{-1} band to disappear (cf. Figure 6). Again, these results correspond to CO-radical destruction as detected by loss of EPR signal. (It should be noted

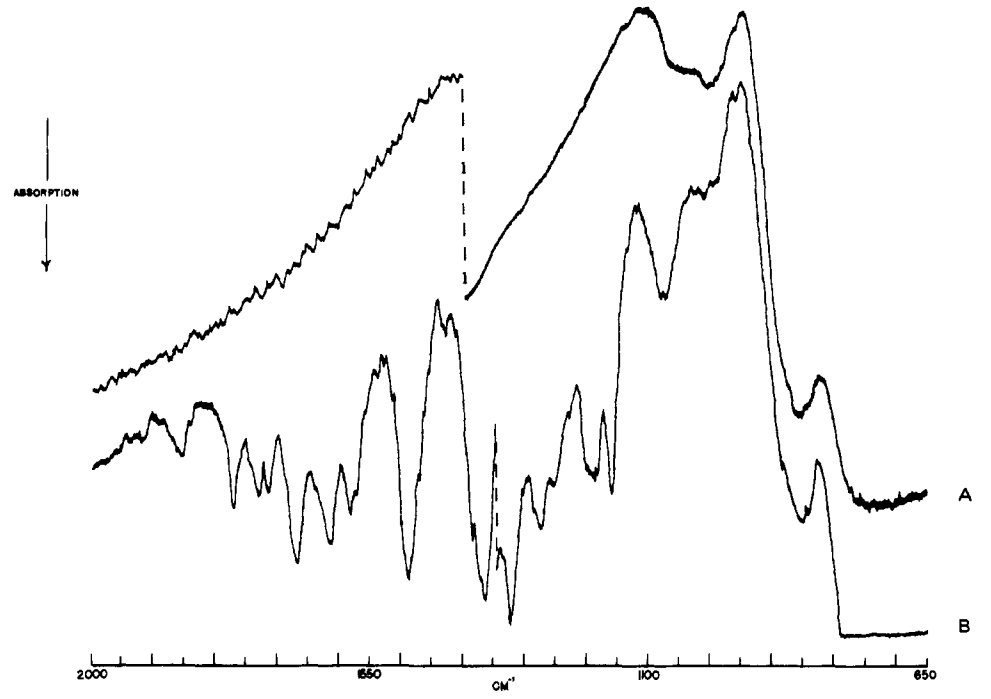

Figure 4. (A) Room temperature infrared spectrum of MgO pre-heated-treated at 720 °C (cm^{-1}); (B) after CO addition (cm^{-1}).

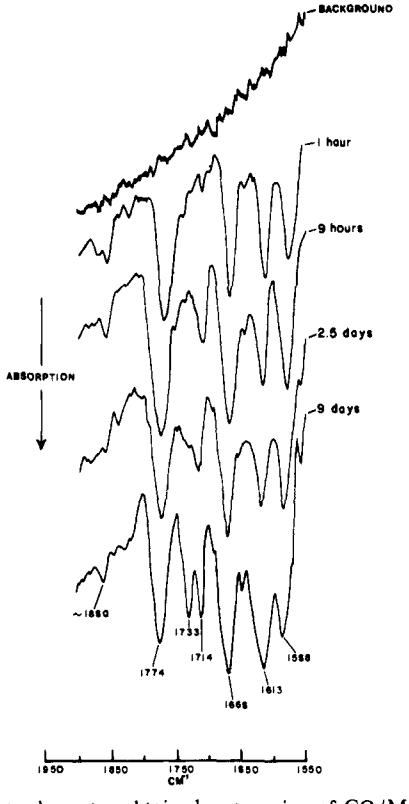

Figure 5. Infrared spectra obtained upon aging of CO/MgO (cm^{-1}). Pre-heat-treatment = 720 °C.

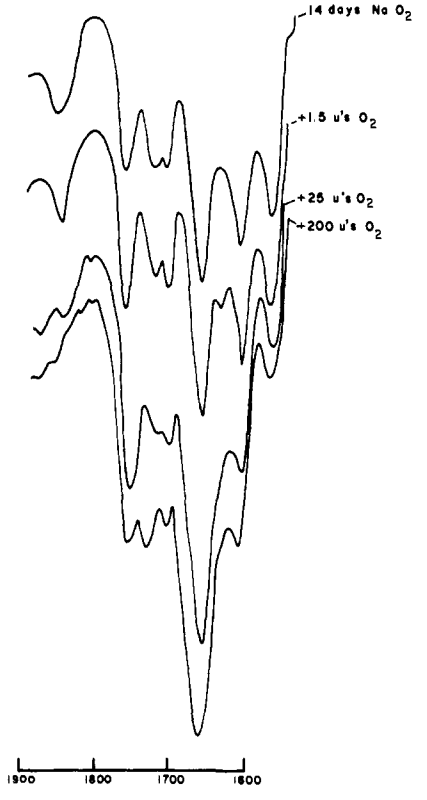

Figure 6. Infrared spectrum of aged CO/MgO after O_2 addition (cm^{-1}, μ = microns pressure of O_2).

that much higher pressures of O_2 cause a new band to grow in about 1750 cm^{-1} which according to Zecchina and co-workers is probably an organic carbonate.)[20]

In light of these data it is very tempting to assign the 1733-cm^{-1} IR band to the CO radical species. The only bothersome consideration is the relatively low intensity of the band assuming that 15% of the CO adsorbed should be in a paramagnetic state. However, the symmetry and surface interactions may serve to greatly affect the absorption properties of the species involved.

If this assignment is indeed correct, there are some significant features that should be pointed out: (1) the CO radical species must possess slightly excess electron density that is manifested in a contribution to the π^* antibonding orbitals of CO; thus the significant lowering of $\nu_{C=O}$ from free $\nu_{C=O}$; (2) alternatively, the CO radical species exists as a bridged structure similar to that described earlier for CO adsorbed on metals[21] (i.e., >C=O). Furthermore it is important to note that no bands above free CO were found in our studies, even though specific efforts to find such bands were made, for ex-

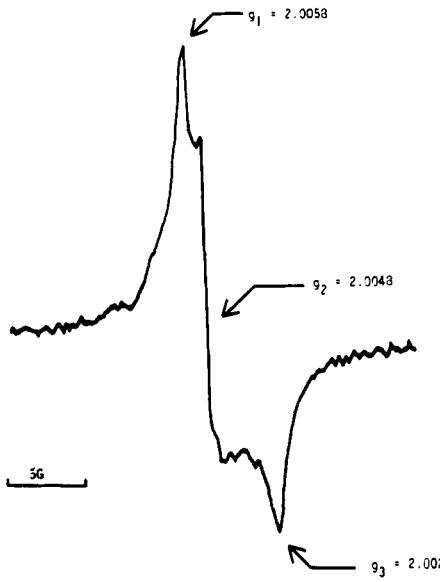

Figure 7. EPR spectrum observed for $^{12}CO/MgO$ (unsymmetrical g tensor).

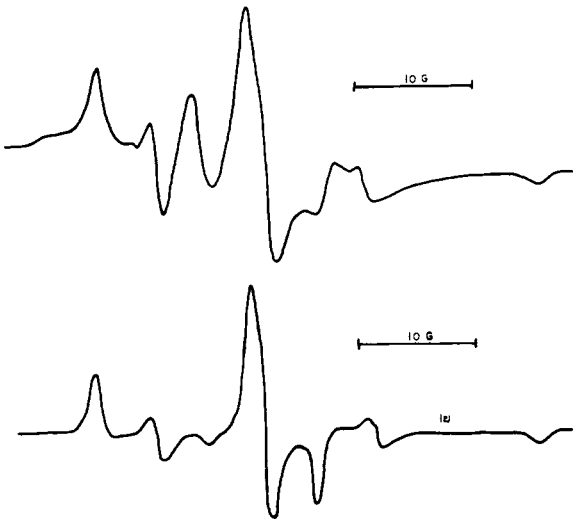

Figure 8. EPR spectrum observed for $^{13}CO/MgO$. (1) Spectrum observed, coupling constants $xx = \pm 3.3$, $yy = \pm 9.4$, and $zz = \pm 19.1$ G; g values $xx = 2.0067$, $yy = 2.0056$, and $zz = 2.0030$. (2) Computer simulation.

ample, purging of all atmospheric CO and CO_2 during IR spectrum recordings.[22] Thus, it appears that no *electron-deficient* adsorbed CO species were present (i.e., $CO^{\delta+}$) since these would be expected to adsorb at very high frequencies, actually *above* free $\nu_{C=O}$.[23]

We conclude from these combined IR-EPR studies that our CO radical species is electron rich and/or in a bridged bonding mode. (See the next section where the dimeric nature of the radical is demonstrated for further discussion of $\nu_{C=O}$ for the radical.)

III. EPR Studies of ^{12}CO and ^{13}CO on MgO. When MgO is thermally activated under vacuum and exposed to CO, a peach color immediately develops. However, the color has little or nothing to do with paramagnetism observed, as radical growth is very slow, comparatively, and it takes 10-60 days for generation of maximum EPR signal.

The EPR spectra indicated that the ^{12}CO radical species exhibited an unsymmetrical g tensor (g_1 = 2.005 80, g_2 = 2.004 80, and g_3 = 2.002 29). There was one sample of MgO, however (MgO II), that showed the same axially symmetric g tensor observed by earlier workers[13] ($g_\perp$ = 2.0058, $g_\parallel$ = 2.0023). The maximum doubly integrated signal intensity observed with the MgO II sample was about the same observed with the other MgO samples. Thus it appears that the differences between the spectra observed are simply due to broadening effects in the case of MgO II, possibly due to iron or other impurities. Analysis did show that MgO II contained at least twice as much iron as the others (cf. Experimental Section). Figure 7 shows the unsymmetrical spectrum normally obtained (with all samples other than MgO II).

Adsorption of ^{13}CO onto heat-treated MgO (not MgO II) yielded a much more complex spectrum as shown in Figure 8. It is important to note that the center portion of the ^{13}CO spectrum possesses a similar line shape as that of a ^{12}CO spectrum. (Recall that the ^{12}CO concentration in ^{13}CO is only 3% of the total.) This observation suggests that the ^{13}CO spectrum contains a center line. By considering this fact in relationship to predicting splitting patterns, it can be concluded that the ^{13}CO radical possesses an even number of equivalent ^{13}C atoms per unpaired electron. In other words, the radical must not be monomeric CO. This conclusion is very interesting when considering that CO telomers on MgO have indeed been detected by reflectance spectroscopy and IR.[19,20] Furthermore, a radical dimer of CO has been postulated to exist on ThO_2.[24]

Owing to the complexity of an unsymmetrical g tensor being split by the anisotropic hyperfine couplings of the ^{13}C, an EPR line simulation computer program (FIBRE) was used as an aid in understanding the observed spectrum. After extensive work with this program it was clear that a monomeric CO radical or polymeric $(CO)_n$ radical where n is 3 or greater could not be responsible for the observed ^{13}CO spectrum. *Only a dimeric structure $(CO)_2$ with the splitting constants shown in Figure 8 gave satisfactory spectral simulations.* This result corroborates the work by Margrave and Krishnan,[25] where CO and Li atoms were codeposited on a cold window. A $(CO)_2^-\cdot Li^+$ species was matrix isolated and characterized spectroscopically. Thus, dimeric radical-anion-like $(CO)_2^-\cdot$ is apparently a reasonably stable molecule.

Currently we are carrying out further experimentation and INDO calculations in order to enable further analysis of the EPR spectra and extract further structural information about the CO dimeric radical.

Conclusions

Based on reactivity comparisons for several thermally activated MgO samples, it can be concluded that similar surface sites are necessary for the production of $C_6H_5NO_2^-\cdot$ and the CO radical species. Based on IR studies of adsorbed CO, including aging, O_2 treatment, and thermal desorption studies, it can be concluded that the CO radical species is electron rich and/or in a bridging bonding mode. Based on ^{13}CO-labeling EPR studies, it can be concluded that the CO radical is dimeric. Overall, it appears that a $(CO)_2^-\cdot$ formulation best describes paramagnetic CO or MgO.

Acknowledgments. The support of R.M.M. through an NSF traineeship is greatly appreciated. This work was supported by the Department of Energy through Contract ERDA-FE, E(49-18)-2211.

References and Notes

(1) Address correspondence to this author at the Department of Chemistry, Kansas State University, Manhattan, Kans. 66056.
(2) See, for example, R. L. Nelson, A. J. Tench, and B. J. Harmsworth, *Trans. Faraday Soc.*, **63**, 1427 (1967).
(3) For a short review see K. J. Klabunde, R. A. Kaba, and R. M. Morris, *Adv. Chem. Ser.*, **No. 173**, 140 (1979).
(4) J. H. Lunsford, *Catal. Rev.*, **8**, 135 (1973).
(5) (a) J. H. Lunsford and J. P. Jayne, *J. Phys. Chem.*, **69**, 2182 (1965); (b) P. Meriaudeau, J. C. Vedrine, Y. B. Taarit, and C. Naccache, *J. Chem. Soc., Faraday Trans. 2*, **71**, 736 (1975); (c) P. Meriaudeau, Y. B. Tarrit, J. C. Vedrine, and C. Naccache, *ibid.*, **73**, 76 (1977).
(6) R. A. Schoonheydt and J. H. Lunsford, *J. Phys. Chem.*, **76**, 323 (1972).

(7) M. J. Lin and J. H. Lunsford, *J. Phys. Chem.*, **80**, 2015 (1976).
(8) A. J. Tench and R. L. Nelson, *Trans. Faraday Soc.*, **63**, 2254 (1967).
(9) D. Cordischi, V. Indovina, and A. Camino, *J. Chem. Soc., Faraday Trans. 1*, **70**, 2189 (1974).
(10) M. Che, C. Naccache, and B. Imelik, *J. Catal.*, **24**, 328 (1972).
(11) T. Iizuka, H. Hattori, Y. Ohno, J. Sohma, and K. Tanabe, *J. Catal.*, **22**, 130 (1971).
(12) K. J. Klabunde, R. A. Kaba, and R. M. Morris, *Inorg. Chem.*, **17**, 2684 (1978).
(13) J. H. Lunsford and J. P. Jayne, *J. Chem. Phys.*, **44**, 1492 (1966).
(14) L. E. Orgel, "Transition Metal Chemistry", Wiley, New York, 1960, pp 135–137.
(15) H. Diehl and G. F. Smith, "Quantitative Analysis", Wiley, New York, 1952, p 366.
(16) F. K. Kneubühl, *J. Chem. Phys.*, **33**, 1074 (1960).
(17) Written by T. Pouemb and E. F. Salde, Quantum Chemistry Program Exchange, Indiana University, Bloomington, Ind. 47401. Parameters are DH = 1.0, Astep = Bstep = 3°.
(18) E. G. Derouane and V. Indovina, *Chem. Phys. Lett.*, **14**, 455 (1972).
(19) (a) A. Zecchina, M. G. Lofthouse, and F. S. Stone, *J. Chem. Soc., Faraday Trans 1*, **71**, 1476 (1975); (b) A. Zecchina and F. S. Stone, *J. Chem. Soc., Chem. Commun.*, 582 (1974); (c) F. S. Stone and A. Zecchina, *Proc. Int. Congr. Catal., 6th*, 162 (1976).
(20) E. Guglielminotti, S. Coluccia E. Garrone, L. Cerruti, and A. Zecchina, *J. Chem Soc., Faraday Trans. 1*, 96 (1979).
(21) (a) R. P. Elschens, W. A. Pliskin, and S. A. Frances, *J. Phys. Chem.*, **60**, 194 (1956); (b) G. Blyholder, *J. Phys. Chem.*, **68**, 2772 (1964); (c) G. A. Ozin, *Acc. Chem. Res.*, **10**, 21 (1977).
(22) Other workers have observed a weak IR band at 2200 cm^{-1}.[20] However, this band could not be due to the paramagnetic species because of its immediate appearance (no aging necessary).
(23) R. H. Hauge, S. E. Gransden, and J. L. Margrave, *J. Chem. Soc., Dalton Trans.*, 745 (1979).
(24) W. S. Brey, Jr., R. B. Gammage, and Y. P. Virmani, *J. Phys. Chem.*, **75**, 895 (1971).
(25) H. Krishnan, Ph.D. Thesis, Rice University, 1975 (with J. L. Margrave).

Photoinsertion of Alkynes into a Ferraborane. Preparation and Characterization of a Novel Tetracarbon Carborane

Thomas P. Fehlner

Contribution from the Department of Chemistry, University of Notre Dame, Notre Dame, Indiana 46556. *Received October 25, 1979*

Abstract: The photolysis of the nido ferraborane, $B_4H_8Fe(CO)_3$, in the presence of an alkyne, RCCR, produces a good yield of the tetracarbon carborane, $R_4C_4B_4H_4$. The *C*-tetramethyl derivative of this new carborane has been characterized primarily by mass and NMR spectroscopy. An intermediate in the formation of this carborane, $(CH_3)_4C_4B_4H_4Fe(CO)_3$, has been isolated and partially characterized. Evidence is also presented for the formation of six- and eight-carbon carboranes in this system. Finally, the photolytic behavior of the ferraborane is contrasted with that of the isoelectronic organometallic compound, $C_4H_4Fe(CO)_3$.

The ability to synthetically modify the size and atom content of heteroborane cages has been a key development behind much of the progress in this area in the last decade.[1] The synthetic methods used have not, in general, included photolysis, although there are some examples of the effective use of photolytic techniques.[2,3] In the work reported below we demonstrate that an iron tricarbonyl fragment in a borane cage constitutes a functional group that, when activated by visible light, facilitates the insertion of alkynes into the borane cage, thereby producing unusual carboranes.[4]

The relationship between boranes and metalloboranes has been explored in detail in recent years.[5] Pertinent to this work is the fact that in many compounds the $Fe(CO)_3$ fragment behaves as a B–H fragment insofar as the geometry of the metalloborane cage is concerned. On the other hand, there are some large differences between boranes and ferraboranes, not the least of which is that the latter absorb in the visible. In fact ferraboranes are light sensitive,[6] suggesting that these compounds may exhibit some useful photochemistry.

As we have previously noted similarities between the filled MO structure of $B_4H_8Fe(CO)_3$ and that of $C_4H_4Fe(CO)_3$[7] and as the latter compound exhibits some interesting photochemistry,[8] we have chosen to first examine the behavior of $B_4H_8Fe(CO)_3$. Pettit and co-workers have demonstrated that the photolysis of cyclobutadieneiron tricarbonyl in the presence of alkynes yields substituted benzenes.[8] Thus, we felt that photolysis of the ferraborane under similar conditions might well yield carboranes. As detailed below, a variety of ferracarboranes and carboranes are produced, although reaction conditions and workup can be chosen such that a single novel tetracarbon carborane can be produced in good yield.

Results and Discussion

Photoactivation of Ferraboranes. The basic features of the electronic structure of ferraboranes as revealed by photoelectron spectroscopy have been discussed previously.[7] Recently, the MO properties of $B_4H_8Fe(CO)_3$ have been explored using SCF $X\alpha$ scattered wave calculations.[9] The nature (energy and atomic composition) of the highest filled MOs of $B_4H_8Fe(CO)_3$ is given in Figure 1 and compared with the highest filled MOs of B_5H_9, the borane analogue of the ferraborane.[10] This comparison emphasizes the fact that the highest lying orbitals in $B_4H_8Fe(CO)_3$ have no counterpart in B_5H_9, are composed mainly of iron 3d atomic functions, and are essentially nonbonding with respect to the cage.[11] The UV–visible spectrum of a methyl derivative of $B_4H_8Fe(CO)_3$ is shown in Figure 2 and the lowest energy absorption is schematically indicated in Figure 1, where it is also compared to that for B_5H_9. As noted in Table I, a variety of ferraboranes and ferracarboranes have lowest energy absorptions in the same energy range and, in all cases, the difference between measured lowest ionization potential and excitation energy is roughly the same. Thus, we suggest that the LUMO in these compounds is also associated with the $Fe(CO)_3$ fragment and irradiation of $B_4H_8Fe(CO)_3$ at 3.1 eV will mainly perturb the $Fe(CO)_3$ fragment. It is well established by work on metal carbonyl systems in general[12] that the absorption of a photon by the metal carbonyl moiety leads to the dissociation of a CO ligand, thereby producing an unsaturated metal center. In the presence of other ligands, this leads to substitution. In the case of $B_4H_8Fe(CO)_2$, ligands such as alkynes may bind to the iron where they are in a potentially reactive position with respect

0002-7863/80/1502-3424$01.00/0